

doi: 10.12029/gc20210522

吴昊,翟庆国,胡培远,唐跃,朱志才,王伟,谢超明,强巴扎西. 2021. 西藏班戈北部早白垩世火山岩:班公湖—怒江洋闭合的岩浆记录[J]. 中国地质, 48(5): 1623–1638.

Wu Hao, Zhai Qingguo, Hu Peiyuan, Tang Yue, Zhu Zhicai, Wang Wei, Xie Chaoming, Qiangba Zhaxi. 2021. Early Cretaceous volcanic rocks in northern Baingoin, Tibet: Magmatic record of the closure of the Bangong–Nujiang Ocean[J]. Geology in China, 48(5): 1623–1638(in Chinese with English abstract).

西藏班戈北部早白垩世火山岩:班公湖—怒江洋闭合的岩浆记录

吴昊¹, 翟庆国¹, 胡培远¹, 唐跃¹, 朱志才¹, 王伟¹, 谢超明², 强巴扎西³

(1. 自然资源部深地动力学重点实验室, 中国地质科学院地质研究所, 北京 100037; 2. 吉林大学地球科学学院, 吉林 长春 130061; 3. 西藏地勘局区域地质调查大队, 西藏 拉萨 851400)

提要:对班戈县北部马前乡地区的早白垩世安山岩和英安岩进行了详细的地质填图及岩石学、年代学、地球化学和Hf同位素研究。锆石U-Pb定年获得安山岩年龄分别为(108.0 ± 1.5) Ma和(113.6 ± 0.9) Ma;英安岩年龄为(106.7 ± 1.9) Ma和(113.6 ± 0.8) Ma。安山岩富集Th和U, 亏损Nb、Ta和Ti, 具有变化范围较大的Mg#值(25~63), 锆石 $\epsilon_{\text{Hf}}(t)$ 值(-8.6~+1.5)以负值为主, 应当为幔源镁铁质熔体与壳源熔体的混合产物。英安岩具有与安山岩类似的微量元素成分特征及负的锆石 $\epsilon_{\text{Hf}}(t)$ 值(-12.3~-8.1), 应当是地壳部分熔融的产物。结合前人研究成果认为, 这些早白垩世岩浆岩是约110 Ma沿班公湖—怒江缝合带岩浆大爆发的产物, 可能与班公湖—怒江洋闭合之后的拉萨与羌塘地块陆—陆碰撞有关。

关 键 词:早白垩世火山岩; 地球化学; 岩石成因; 岩浆混合; 地质调查工程; 班公湖—怒江缝合带

中图分类号:P588.142; P588.144 **文献标志码:**A **文章编号:**1000-3657(2021)05-1623-16

Early Cretaceous volcanic rocks in northern Baingoin, Tibet: Magmatic record of the closure of the Bangong–Nujiang Ocean

WU Hao¹, ZHAI Qingguo¹, HU Peiyuan¹, TANG Yue¹, ZHU Zhicai¹,
WANG Wei¹, XIE Chaoming², QIANGBA Zhaxi³

(1. Key Laboratory of Deep-Earth Dynamics of Ministry of Natural Resources, Institute of Geology, Chinese Academy of Geological Sciences, Beijing 100037, China; 2. College of Earth Science, Jilin University, Changchun 130061, Jilin, China; 3. Regional Geological Survey Party, Tibet Bureau of Geology and Mineral Exploration and Development, Lhasa 851400, Tibet, China)

Abstract: The petrological, zircon U–Pb dating, whole-rock geochemical, and zircon Hf isotopic data of the Early Cretaceous

收稿日期:2019-08-14; 改回日期:2019-12-23

基金项目:国家自然科学基金项目(42072268、42002069、41872240)、第二次青藏高原综合科学考察(2019QZKK0703)和中国地质调查局项目(DD20190370、DD20190060)联合资助。

作者简介:吴昊,男,1993年生,硕士,构造地质学专业;E-mail:2757717424@qq.com。

通讯作者:翟庆国,男,1980年生,研究员,博士生导师,从事青藏高原区域构造与大地构造研究;E-mail:zhaiqingguo@126.com。

andesites and dacites in the Maqianxiang area of Baigoin County, Tibet, are reported. The zircon U-Pb ages of andesite are (108.0 ± 1.5) Ma and (113.6 ± 0.9) Ma, and those of dacite are (106.7 ± 1.9) Ma and (113.6 ± 0.8) Ma. The andesites are enriched in Th and U and depleted in Nb, Ta, and Ti, have variable Mg[#] values (25–63), and show mainly negative zircon $\varepsilon_{\text{Hf}}(t)$ values (-8.6 to $+1.5$). They are probably generated by mixing of mantle- and crust-derived melts. Dacite shares similar trace element features with the coeval andesite, and has negative zircon $\varepsilon_{\text{Hf}}(t)$ values (-12.3 to -8.1). It is interpreted as a product of partially melting crust. The andesite and dacite are interpreted as a product of the ca.110 Ma magmatism along the Bangong–Nujiang suture zone, and may be related to the continent–continent collision process after the closure of the Bangong–Nujiang Ocean.

Key words: Early Cretaceous volcanics; geochemistry; petrogenesis; magma mixing; geological survey engineering; Bangong–Nujiang suture zone; Tibet

About the first author: WU Hao, male, born in 1993, master candidate, majoring in structural geology; E-mail:2757717424@qq.com.

About the corresponding author: ZHAI Qingguo, male, born in 1980, Ph.D supervisor, engaged in the research on regional structure of Tibet Plateau and geotectonics; E-mail: zhaiqingguo@126.com.

Fund support: Suported by National Natural Science Foundation (No.14072268, No.42002069, No.41872240), The Second Comprehensive Scientific Investigation of the Tibetan Plateau (No. 2019QZKK0703), and China Geological Survey Program (No. DD20190370, No. DD20190060).

1 引言

青藏高原记录了特提斯洋以及印度—亚洲大陆的聚合、碰撞造山的地质演化过程,是当今地球科学研究的热点和前沿(侯增谦等,2004,2006;许志琴等,2006,2016;杨经绥等,2004;李海兵等,2006;赵慧等,2015)。班公湖—怒江缝合带横亘于青藏高原中部,记录了班公湖—怒江中特提斯洋的俯冲消减以及拉萨地块和南羌塘地块的碰撞过程,是研究中特提斯洋从洋—陆俯冲到陆—陆碰撞演化历史的关键。

截至目前,班公湖—怒江缝合带的研究依然存在较多争议,很多关键科学问题尚未解决,尤其是班公湖—怒江中特提斯洋的闭合时间(Girardeau et al., 1984; Kapp et al., 2007; Hu et al., 2017)。当前主要分为两种观点,一种观点认为,班公湖—怒江洋盆一直持续到晚白垩世才发生闭合(朱弟成等,2006; Zhang et al., 2004, 2012; Fan et al., 2014; Wu et al., 2015; Liu et al., 2018),主要证据为早白垩世晚期($120\sim108$ Ma)的“洋岛型”岩石组合(包括OIB型玄武岩和伴生的灰岩)(Zhu et al., 2006; Liu et al., 2014; Zhang et al., 2014; Fan et al., 2015)。另一种观点认为,班公湖—怒江特提斯洋在早白垩世之前就已经闭合并进入陆—陆碰撞阶段(Xu et al., 1985; Guynn et al., 2006; Kapp et al., 2007; Leier et al., 2007; Chen et al., 2015, 2017a),主要依据古地磁(Matte et al., 1996; Lippert et al., 2014; Zhu et al.,

2015)和沉积学(Kapp et al., 2007)方面的证据。

近年来的研究显示,在班公湖—怒江缝合带内部及两侧出露有大量早白垩世中酸性火山岩和花岗岩(Zhu et al., 2009),它们可以为研究班公湖—怒江特提斯洋的演化历史提供重要约束。本文报道了新近在班公湖—怒江缝合带中段班戈县马前乡地区的早白垩世去申拉组安山岩和英安岩。在野外填图的基础上,对这些岩石开展了系统的岩石学、地球化学和锆石U-Pb年代学研究工作。结合班公湖—怒江缝合带内已有同期岩浆岩的资料,本文讨论了马前乡地区早白垩世火山岩的岩浆源区和岩石成因,及其对班公湖—怒江中特提斯洋的闭合时间的约束。

2 地质概况

青藏高原是研究大陆动力学和板块构造理论的天然实验室。前人研究表明,青藏高原由一系列的陆块和缝合带组成。这些陆块包括昆仑、北美塘、南羌塘、拉萨和喜马拉雅地块,这些地块被金沙江缝合带、龙木错—双湖—澜沧江缝合带、班公湖—怒江缝合带和雅鲁藏布江缝合带分割(图1a)。

研究区位于班公湖—怒江缝合带中段,行政规划属于班戈县马前乡(图1a),大地构造上处在拉萨地块北缘火山岩浆弧带中。研究区出露的地层主要为三叠系、侏罗系、白垩系和古近系(图1b)。三叠系主要为上三叠统确哈拉群(T_3q),岩性以细砂岩

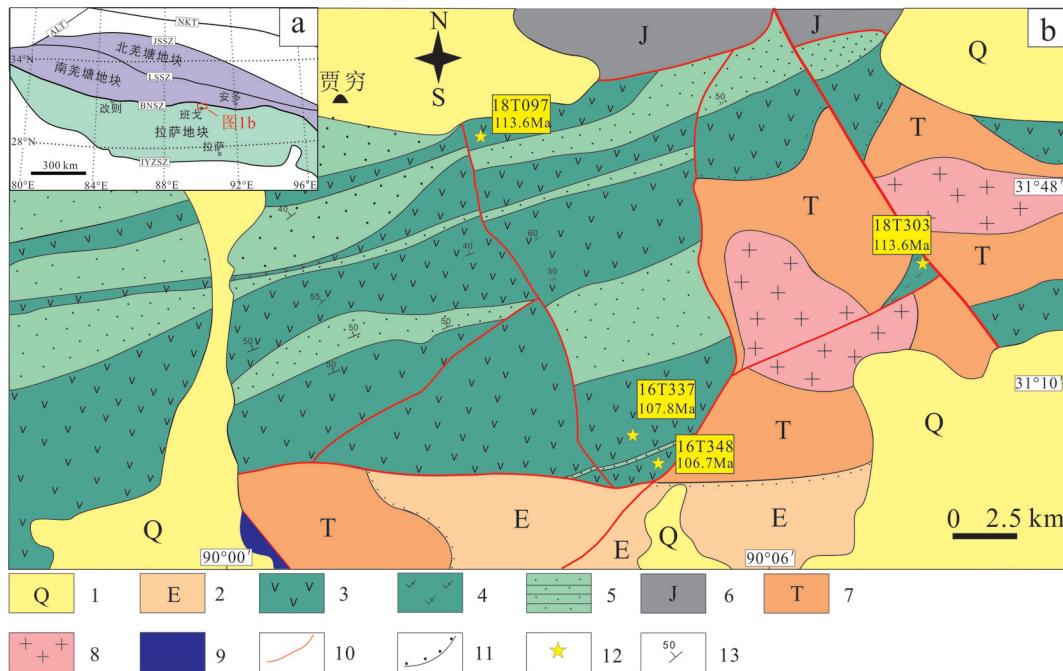


图1 青藏高原构造划分简图(a, 据Hu et al., 2017)和西藏班戈县马前乡地区地质简图(b)

BNSZ—班公湖—怒江缝合带; LSSZ—龙木错—双湖缝合带; IYZSZ—雅鲁藏布江缝合带; JSSZ—金沙江缝合带; 1—第四系; 2—古近系牛堡组; 3—白垩系去申拉组安山岩; 4—白垩系去申拉组英安岩; 5—白垩系去申拉组砂岩; 6—侏罗系接奴群; 7—三叠系确哈拉群; 8—三叠纪花岗岩; 9—蛇绿岩; 10—断层; 11—不整合接触; 12—年龄采样点; 13—产状

Fig.1 Tectonic framework of the Tibetan Plateau (a, after Hu et al., 2017) and simplified geological map (b) of Maqian Town, Banggoin County

BNSZ—Bangong Co-Nujiang suture zone; LSSZ—Longmu Co-Shuanghu suture zone; IYZSZ—Yarlung Zangbo suture zone; JSSZ—Jinshajiang suture zone; 1—Quaternary; 2—The Paleogene Niubao Formation; 3—The Cretaceous andesite of Qushenla Formation; 4—The Cretaceous dacite of Qushenla Formation; 5—The Cretaceous sandstone of Qushenla Formation; 6—The Jurassic Jieu Group; 7—The Triassic Quehala Group; 8—The Triassic granite; 9—Ophiolite; 10—Fault; 11—Unconformable contact; 12—Sampling site; 13—Occurrence

和含砾粗砂岩为主,二者呈互层状产出,顶部发育薄层灰岩。侏罗系主要为中上侏罗统接奴群($J_{2-3}jn$),以变质粉砂岩、变质砂岩和灰黑色板岩为主,与下白垩统去申拉组(K_1q)以断层相接触。白垩系去申拉组不整合覆盖于确哈拉群之上,岩性主要为安山岩、英安岩、砂岩和少量火山碎屑岩,其中安山岩与砂岩多呈互层状产出。古近系主要是牛堡组($E_{1-2}n$)红层,岩性以中—厚层状砂岩和砾岩为主。

3 岩石学特征

本文采集的火山岩样品来自于去申拉组,岩石类型包括安山岩和英安岩,采样位置见图1b,样品包括4件同位素测年样品和28件岩石和地球化学样品,其中典型样品的岩石学特征如下:

安山岩:呈灰色、深灰色,斑状结构,块状构造(图2f)。斑晶总含量约占20%,主要为斜长石(约60%)、角闪石(约25%)、辉石(约10%)和少量黑云

母(约5%)。斜长石呈板柱状,长度为50~2000 μm,发育聚片双晶(图2h),部分发生了蚀变作用而形成绢云母。辉石呈板状,长度为100~2000 μm,斜消光,消光角为40°,部分发生了绿泥石化和绿帘石化。角闪石多呈长柱状和粒状,部分蚀变。黑云母呈片状(0.2~0.7 mm),一组极完全解理,平行消光,有的具暗化边结构,部分蚀变。基质主要为斜长石微晶、暗色矿物。

英安岩:灰绿色,具斑状结构,块状构造(图2g)。斑晶占10%~15%,由斜长石和少量石英组成。斜长石为自形—半自形板柱状,石英斑晶呈现珍珠光泽,基质为隐晶质,多为微晶或针状长石类矿物和暗色矿物。

4 分析方法

锆石U-Pb测年样品中锆石的分选在河北省区域地质调查队实验室完成,采用常规的重液和磁选

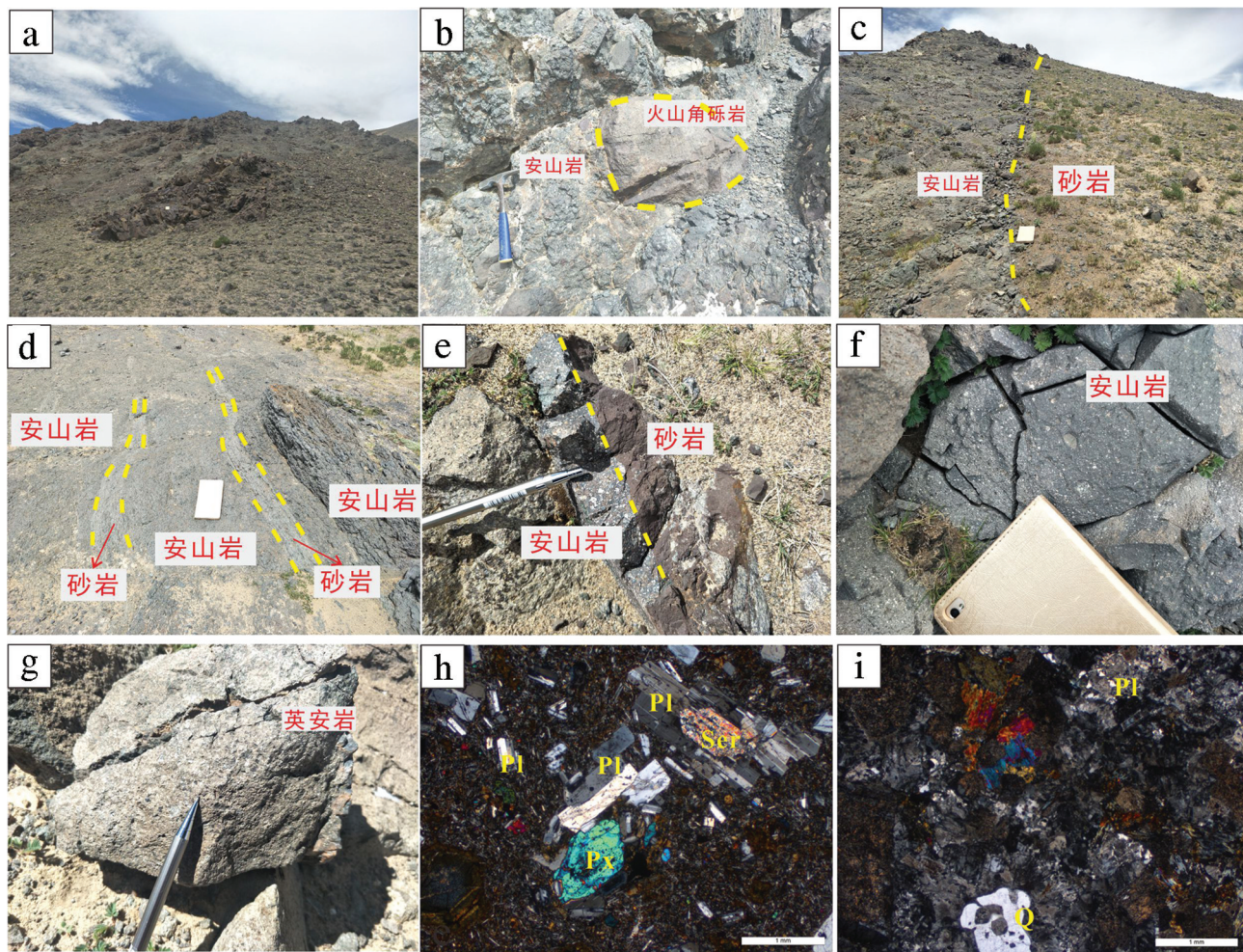


图2 西藏班戈县马前乡火山岩野外露头及显微照片

a—安山岩远景; b—安山岩夹火山角砾岩;c, d, e—火山岩与砂岩界限; f—安山岩近景; g—英安岩近景; h—安山岩镜下照片; i—英安岩镜下照片; Pl—斜长石; Px—辉石; Ser—绢云母; Q—石英

Fig. 2 Field photographs and microphotographs of the volcanic rocks in Maqian Town of Baingoin County, Tibet

a—Distant view of andesites; b—Andesites intermingled with volcanic breccia; c,d,e—The boundary between volcanic rock and sandstone; f—Tight shot of andesites; g—Tight shot of dacites; h—Microphotographs of andesites; i— Microphotographs of dacites; Pl—Plagioclase; Px—Pyroxene; Ser—Sericite; Q—Quartz

方法进行分选,最后在双目显微镜下挑纯。样品靶的制备在中国地质科学院地质研究所完成,制成的样品靶直径为25 mm。锆石的阴极荧光图像分析在中国地质科学院地质研究所的阴极荧光分析系统(HITACH S-3000N型场发射环境扫描电镜和Gatan公司Chroma阴极荧光谱仪)上完成。样品的锆石U-Th-Pb分析在北京科荟测试技术有限公司完成,分析仪器为美国ESI公司生产的NWR 193 nm激光剥蚀进样系统和德国AnlyitikJena公司生产的PQMS Elite型四级杆等离子体质谱仪联合构成的激光等离子体质谱仪(LA-ICP-MS)。本次分析193 nm激光器工作频率为10 Hz;测试点束斑直径

为25 μm ,剥蚀采样时间为45 s,具体分析流程见相关文献(侯可军等,2009)。锆石GJ-1(Jackson et al., 2004)作为外部标准来校正分析过程中的同位素分馏;NIST610作为外部标准来获得分析点的Th和U的含量。锆石U-Pb年龄用ICPMSDataCal数据处理软件(Liu et al., 2010)计算获得,加权平均年龄的计算和谐和图的绘制采用ISOPLOT 3.0程序(Ludwig et al., 2003)。锆石Hf同位素分析也在北京科荟测试技术有限公司完成,在Neptune Plus多接收电感耦合等离子质谱仪(MC-ICPMS)和NWR 213 nm激光取样系统上进行,分析中,标准锆石 $^{176}\text{Hf}/^{177}\text{Hf}$ 比值范围为 0.282496 ± 9 ($2\sigma, n=276$),

仪器的运行条件及详细的分析过程参见相关文献(Wu et al., 2006)。采用单点剥蚀模式,斑束固定为44 μm。全岩主量、微量元素和稀土元素的分析在国家地质实验测试中心。主量元素采用X-射线荧光光谱仪(PW4400)分析。微量元素和稀土元素的分析仪器为X-series等离子质谱仪,实验室分析详细方法见相关文献(Hu et al., 2018)。

5 分析结果

5.1 锆石U-Pb年龄

西藏班戈北部马前乡地区岩浆岩的4件样品的锆石定年结果见表1。

安山岩样品16T337和18T097中的锆石呈短柱状,自形—半自形,粒径范围在100~150 μm,具有明显的岩浆振荡环带(图3a、b)。锆石Th/U值分别介于0.74~2.41和0.40~1.03,表明这些锆石属于岩浆成因锆石。在U-Pb年龄谐和图上,分析点均落在曲线上及附近,测点的²⁰⁶Pb/²³⁸U年龄范围分别为106~109 Ma和110~114 Ma,年龄加权平均值分别为(108.0±1.5)Ma(MSWD=0.072)和(113.6±0.9)Ma(MSWD=0.20),代表了安山岩的岩浆结晶年龄。

英安岩样品16T348和18T303中的锆石多呈长柱状,自形,粒度较安山岩小,粒径范围在50~100 μm,锆石有明显的岩浆振荡环带(图3c)。锆石Th/U比值分别在0.60~1.31和1.03~1.98(>0.1),显示出典型岩浆锆石的特征,测点的²⁰⁶Pb/²³⁸U年龄变化范围分别为(105~109) Ma和113~114 Ma,加权平均值分别为(106.7±1.9) Ma(MSWD=0.23)和(113.6±0.8) Ma(MSWD=0.042),代表了英安岩的岩浆结晶时代。

5.2 全岩地球化学

28件样品主全岩主量、微量元素和稀土元素分析结果见表2。如前文所述,样品发生了不同程度的后期蚀变作用,显示出较高、且变化范围较大的烧失量(1.31%~5.90%),因此,Ba、K、Na、Pb、Rb、Sr、U等活动性元素不宜用来探讨岩石成因及其形成的大地构造环境。通常认为,高场强元素(如Nb、Ta、Zr、Hf等)、相容元素(如Cr、Ni)和稀土元素受蚀变作用的影响较小,本文主要根据这些元素的组成特征,讨论火山岩的类型和成因等(Winchester and Floyd, 1977; Hastie et al., 2007)。

安山岩样品主要的氧化物质量分数及比值如

下:SiO₂为52.77%~63.40%,Al₂O₃为14.86%~18.73%,MgO为0.63%~5.27%,K₂O为0.73%~2.53%,K₂O/Na₂O为0.18~0.69,TiO₂为0.76%~0.98%。其中,部分样品的MgO含量较高(表2),与高镁安山岩类似。在Zr/TiO₂*0.0001-SiO₂图解上(图4a),样品投点主要落在安山岩的区域内。在Co-Th图解中(图4b),样品点位于高钾钙碱性岩石区域。稀土元素含量较高(Σ REE=96×10⁻⁶~149×10⁻⁶),球粒陨石标准化稀土元素配分曲线(图5b)呈轻稀土元素富集、重稀土元素亏损的右倾模式((La/Yb)_N=4.78~8.08),并且具有弱的Eu负异常(Eu/Eu*=0.72~0.85)。在原始地幔标准化微量元素蛛网图(图5a)上,样品具有明显富集Th和U,亏损Nb、Ta和Ti的特征,这与典型岛弧火山岩类似。

英安岩样品主要的氧化物质量分数如下:Al₂O₃为14.40%~16.05%,MgO为0.52%~1.93%,K₂O为1.47%~44.42%,TiO₂为0.52%~0.73%。与安山岩样品相比,英安岩样品具有较高的SiO₂含量,为62.03%~67.86%。在SiO₂-Zr/TiO₂*0.0001图解中(图4a),样品投点主要落在流纹英安岩/英安岩的区域内。在Co-Th图解中(图4b),样品点全部位于高钾钙碱性系列岩石的范围内。稀土元素球粒陨石标准化配分曲线(图5d)呈轻稀土元素富集、重稀土元素亏损的右倾模式,具有弱的Eu负异常(Eu/Eu*=0.42~0.78)。英安岩与安山岩样品呈现出类似的微量元素成分特征(图5c),均富集Th和U,亏损Nb、Ta和Ti。

5.3 锆石Hf同位素

本项研究对所有测年锆石进行Hf同位素分析,共获得了43个锆石的测试数据,分析点均在锆石U-Pb定年的原位或相邻部位进行,数据结果见表3。安山岩样品中锆石的初始¹⁷⁶Hf/¹⁷⁷Hf比值为0.282545~0.282658,锆石 $\varepsilon_{\text{Hf}}(t)$ 值(-8.6~+1.5)以负值为主(图6),对应的二阶段模式年龄(T_{DM}^{C})为1069~1712 Ma。英安岩样品中锆石的初始¹⁷⁶Hf/¹⁷⁷Hf比值为0.282356~0.282474,对应的锆石 $\varepsilon_{\text{Hf}}(t)$ 值在-12.3~-8.1(图6),二阶段模式年龄(T_{DM}^{C})为1748~1952 Ma。

6 讨论

6.1 去申拉组火山岩的形成时代

去申拉组火山岩断续分布于班公湖—怒江缝

表1 西藏班戈县马前乡火山岩锆石U-Th-Pb同位素数据

Table 1 LA-ICP-MS zircon U-Th-Pb data of the volcanic rocks in Maqian Town of Baingoin County, Tibet

测点	Pb /10 ⁻⁶	U /10 ⁻⁶	Th /10 ⁻⁶	²³² Th / ²³⁸ U	²⁰⁷ Pb / ²⁰⁶ Pb	±%	²⁰⁷ Pb / ²³⁵ U	±%	²⁰⁶ Pb / ²³⁸ U	±%	²⁰⁷ Pb/ ²⁰⁶ Pb Age /Ma	²⁰⁷ Pb/ ²³⁵ U Age /Ma	²⁰⁶ Pb/ ²³⁸ U Age /Ma	
16T337, 安山岩														
3	18	950	646	1.50	0.0482	0.0024	0.1138	0.0067	0.0170	0.0004	109	124	109	6.1
4	13	676	475	1.42	0.0473	0.0031	0.1120	0.0084	0.0170	0.0004	65	156	108	7.7
7	28	1405	982	1.43	0.0483	0.0021	0.1135	0.0066	0.0170	0.0005	122	-93	109	6.0
8	25	794	1069	0.74	0.0485	0.0015	0.1121	0.0040	0.0169	0.0004	124	72	108	3.6
11	29	1569	1002	1.57	0.0494	0.0017	0.1157	0.0048	0.0169	0.0004	169	84	111	4.4
13	33	1055	2236	2.12	0.0474	0.0017	0.1106	0.0045	0.0169	0.0004	78	76	107	4.1
15	34	2236	1055	2.41	0.0474	0.0017	0.1106	0.0045	0.0169	0.0004	78	76	107	4.1
19	67	4861	2017	0.75	0.0487	0.0009	0.1129	0.0028	0.0169	0.0004	132	44	109	2.6
21	23	700	937	1.23	0.0491	0.0019	0.1151	0.0050	0.0170	0.0004	154	93	110	4.4
23	19	851	690	0.81	0.0483	0.0025	0.1110	0.0063	0.0166	0.0004	122	109	107	5.7
18T097, 安山岩														
1	13	257	636	0.40	0.0488	0.0025	0.1211	0.0067	0.0179	0.0003	139	122	116	6.0
3	11	469	488	0.96	0.0497	0.0020	0.1211	0.0044	0.0178	0.0003	189	125	116	4.0
4	8	274	362	0.76	0.0506	0.0038	0.1244	0.0100	0.0178	0.0004	233	172	119	9.0
5	9	388	419	0.92	0.0462	0.0021	0.1131	0.0054	0.0178	0.0003	9	107	109	4.9
6	10	372	440	0.85	0.0502	0.0053	0.1228	0.0125	0.0179	0.0004	206	230	118	11.3
8	10	327	450	0.73	0.0468	0.0027	0.1154	0.0071	0.0178	0.0002	39	137	111	6.5
11	12	342	549	0.62	0.0478	0.0019	0.1166	0.0046	0.0178	0.0002	87	102	112	4.2
13	13	362	628	0.58	0.0469	0.0029	0.1151	0.0078	0.0178	0.0005	43	141	111	7.2
14	9	376	404	0.93	0.0476	0.0049	0.1174	0.0127	0.0179	0.0004	80	230	113	11.6
15	8	313	362	0.86	0.0506	0.0053	0.1214	0.0110	0.0178	0.0004	220	235	116	9.9
16	10	326	409	0.80	0.0709	0.0054	0.1736	0.0129	0.0179	0.0003	953	156	163	11.1
17	11	441	471	0.94	0.0495	0.0023	0.1202	0.0055	0.0177	0.0002	169	109	115	5.0
18	10	401	474	0.85	0.0490	0.0041	0.1177	0.0115	0.0173	0.0003	146	185	113	10.4
21	14	5544	578	0.96	0.0707	0.0073	0.1730	0.0183	0.0177	0.0003	950	213	162	15.8
25	11	505	489	1.03	0.0473	0.0022	0.1157	0.0052	0.0178	0.0002	61	107	111	4.7
16T348, 黄安岩														
2	31	1408	1199	1.17	0.0474	0.0026	0.1120	0.0072	0.0170	0.0004	78	117	108	6.6
8	17	443	743	0.60	0.0501	0.0025	0.1141	0.0050	0.0167	0.0003	211	121	110	4.6
11	30	1209	1227	0.99	0.0501	0.0031	0.1132	0.0069	0.0164	0.0004	198	142	109	6.3
12	16	610	656	0.93	0.0483	0.0042	0.1122	0.0116	0.0166	0.0004	122	183	108	10.6
14	73	2632	2991	0.88	0.0496	0.0014	0.1158	0.0057	0.0168	0.0005	176	69	111	5.2
21	17	724	707	1.02	0.0492	0.0044	0.1135	0.0105	0.0166	0.0003	154	196	109	9.6
22	23	1193	912	1.31	0.0495	0.0030	0.1139	0.0075	0.0168	0.0005	172	136	110	6.8
18T303, 黄安岩														
1	5	197	279	1.42	0.0476	0.0034	0.1151	0.0080	0.0177	0.0003	80	163	111	7.3
2	9	377	429	1.14	0.0487	0.0037	0.1198	0.0093	0.0179	0.0004	132	174	115	8.4
3	15	608	866	1.42	0.0490	0.0033	0.1171	0.0070	0.0179	0.0004	146	148	112	6.3
4	8	330	416	1.26	0.0485	0.0033	0.1190	0.0086	0.0178	0.0003	120	152	114	7.8
5	7	280	326	1.16	0.0491	0.0031	0.1189	0.0074	0.0177	0.0003	150	144	114	6.8
7	7	263	294	1.12	0.0518	0.0032	0.1264	0.0079	0.0179	0.0003	276	143	121	7.1
9	12	434	859	1.98	0.0503	0.0029	0.1230	0.0072	0.0177	0.0003	209	131	118	6.5
10	7	296	326	1.10	0.0476	0.0036	0.1162	0.0086	0.0178	0.0003	80	170	112	7.8
11	12	456	700	1.53	0.0505	0.0031	0.1234	0.0076	0.0178	0.0003	217	138	118	6.9
12	9	360	427	1.19	0.0466	0.0044	0.1120	0.0097	0.0177	0.0005	33	206	108	8.9
13	9	380	451	1.18	0.0507	0.0042	0.1228	0.0098	0.0177	0.0003	228	188	118	8.9
14	9	359	428	1.19	0.0529	0.0051	0.1267	0.0111	0.0177	0.0003	324	214	121	10.0
15	12	464	618	1.33	0.0510	0.0023	0.1238	0.0052	0.0179	0.0003	239	104	118	4.7
16	6	243	312	1.28	0.0504	0.0037	0.1217	0.0086	0.0177	0.0004	213	170	117	7.7
17	6	255	273	1.07	0.0549	0.0030	0.1351	0.0078	0.0178	0.0002	409	124	129	7.0
18	10	381	483	1.27	0.0469	0.0023	0.1132	0.0047	0.0178	0.0003	56	111	109	4.3
19	10	344	612	1.78	0.0502	0.0029	0.1222	0.0069	0.0178	0.0003	211	142	117	6.3
20	6	265	303	1.14	0.0531	0.0040	0.1295	0.0097	0.0178	0.0003	332	172	124	8.7
21	11	404	658	1.63	0.0512	0.0033	0.1248	0.0080	0.0178	0.0004	250	145	119	7.3
22	14	519	820	1.58	0.0503	0.0027	0.1237	0.0067	0.0178	0.0002	209	126	118	6.0
23	8	309	340	1.10	0.0503	0.0026	0.1220	0.0063	0.0177	0.0003	209	119	117	5.7
24	7	302	312	1.03	0.0500	0.0044	0.1224	0.0112	0.0177	0.0004	198	193	117	10.1
25	5	225	259	1.15	0.0480	0.0037	0.1180	0.0097	0.0179	0.0004	98	174	113	8.8

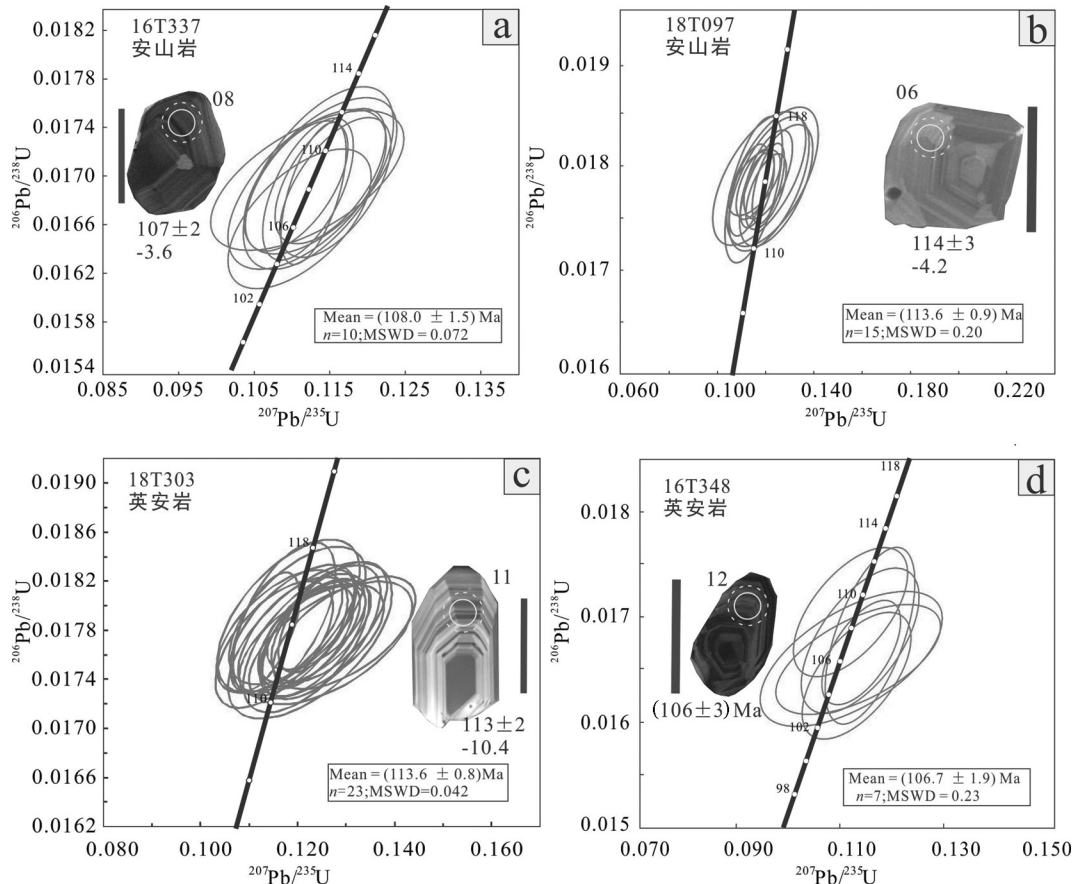


图3 西藏班戈县马前乡安山岩(a,b)和英安岩(c,d)的LA-ICP-MS锆石U-Pb谐和图(比例尺代表100 μm)

Fig. 3 LA-ICP-MS zircon U-Pb concordant diagrams of the andesite (a, b) and dacite (c, d) in Maqian Town of Baingoin County, Tibet (The scale bar on the CL images representing 100 μm)

合带中,是探索该缝合带构造演化过程的重要载体。陈玉禄(2002)最早在班戈一切里错地区对去申拉组进行了岩石学的论述,同时获126 Ma的全岩Rb-Sr同位素年龄值,从而初步证实去申拉组火山岩时代为早白垩世。吴浩等(2013)对塔色普勒地

区的去申拉组火山岩进行了地球化学和年代学研究,认为其形成的地球动力学背景是早白垩世晚期班公湖—怒江洋壳南向俯冲过程中发生的板片分离,并指示该地区班公湖—怒江洋的陆—陆碰撞时间在107 Ma左右。朱弟成等(2006)对该期火山活

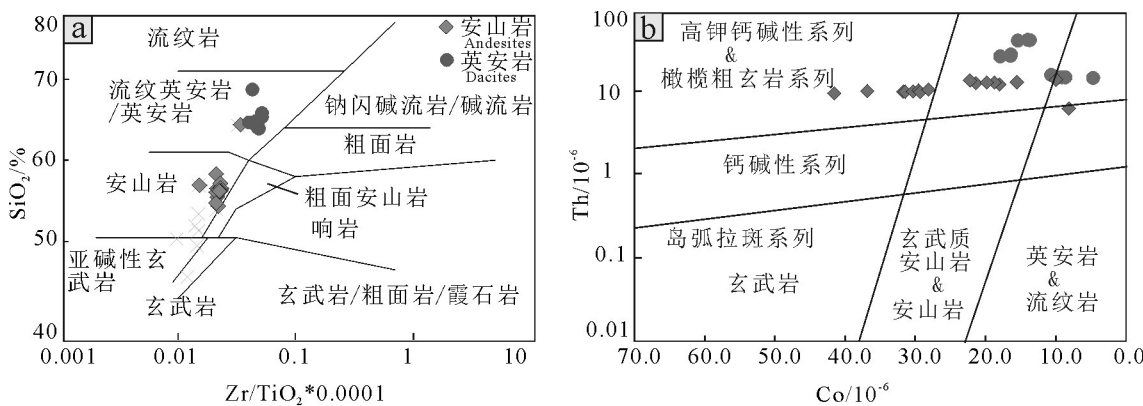


图4 西藏班戈县马前乡火山岩的Zr/TiO₂*0.0001-SiO₂(a)和Co-Th图解(b)

Fig.4 Zr/TiO₂*0.0001-SiO₂(a) and Co-Th diagrams (b) of the volcanic rocks in Maqian Town of Baingoin County, Tibet

表2 西藏班戈县马前乡火山岩主量(%)和微量元素(10^{-6})成分分析结果Table 2 Major (%) and trace (10^{-6}) elements data of the volcanic rocks in the Maqianxiang area, Baingoin County, Tibet

样品号	16T337	16T338	16T339	16T340	16T341	16T342	16T343	16T344	16T345
岩性	安山岩								
SiO ₂	56.75	56.70	55.94	56.07	56.25	56.67	53.47	56.55	55.00
TiO ₂	0.76	0.77	0.78	0.78	0.77	0.76	0.78	0.79	0.78
Al ₂ O ₃	15.02	14.86	15.07	15.2	15.3	15.08	15.31	15.35	15.21
TFeO	6.59	6.41	6.01	6.63	6.29	6.13	5.79	6.39	6.18
TFe ₂ O ₃	7.32	7.12	6.67	7.36	6.99	6.80	6.43	7.10	6.86
MnO	0.10	0.10	0.11	0.12	0.10	0.11	0.16	0.10	0.13
MgO	5.27	4.63	4.40	4.80	4.75	3.99	4.10	4.48	3.62
CaO	7.95	8.80	9.36	8.13	8.84	8.54	10.44	8.31	9.33
Na ₂ O	2.78	2.64	2.70	2.75	2.70	2.73	2.69	2.76	2.65
K ₂ O	1.71	1.61	1.51	1.67	1.61	1.67	1.45	1.65	1.49
P ₂ O ₅	0.14	0.14	0.14	0.14	0.14	0.14	0.14	0.15	0.14
LOI	1.94	2.95	2.93	2.16	2.77	3.03	4.69	2.42	4.08
总计	99.74	100.32	99.61	99.18	100.22	99.52	99.66	99.66	99.29
Li	18.70	22.10	20.80	19.10	19.90	20.90	32.80	22.20	28.70
Be	1.39	1.47	1.41	1.46	1.49	1.33	1.42	1.38	1.45
Sc	21.10	20.50	23.00	21.40	22.50	22.80	24.60	23.90	23.30
V	158	156	166	163	164	180	196	195	190
Cr	352	323	389	246	363	300	366	289	298
Co	29.40	29.50	31.70	30.30	31.40	28.10	41.50	30.30	36.80
Ni	52.70	53.00	58.40	51.80	55.50	48.60	57.20	52.80	53.00
Ga	16.50	16.10	16.60	17.30	16.80	16.20	16.50	16.70	16.70
Rb	60.50	54.90	53.70	60.90	56.40	59.60	50.60	57.80	53.10
Sr	259	259	267	278	271	258	263	261	276
Zr	168	164	167	173	167	166	159	173	170
Nb	7.72	7.60	7.82	8.04	7.73	7.88	7.56	7.87	7.97
Cs	3.68	3.43	2.55	3.40	3.46	3.68	1.79	2.58	2.82
Ba	304	284	276	296	284	298	262	296	276
Ta	0.58	0.56	0.57	0.58	0.57	0.59	0.57	0.58	0.60
Pb	25.40	30.90	14.00	20.50	32.00	16.20	128	14.20	130
Th	9.36	9.79	9.57	9.51	9.42	9.98	9.07	9.49	9.62
U	1.80	1.86	1.80	1.81	1.78	1.82	1.67	1.75	1.81
Y	22.60	22.10	22.50	24.00	22.60	21.70	21.60	21.90	22.40
Ti	4898	4887	5171	5205	5163	4877	5007	5201	5109
La	24.20	24.00	23.90	24.40	23.60	24.90	23.40	24.30	25.00
Ce	46.90	47.50	46.80	47.60	46.20	47.40	43.80	46.50	47.30
Pr	5.20	5.21	5.15	5.34	5.21	5.42	5.05	5.37	5.42
Nd	19.80	20.00	20.10	20.30	20.00	21.40	20.50	21.30	21.70
Sm	4.23	4.24	4.28	4.43	4.34	4.30	4.11	4.28	4.38
Eu	1.05	1.06	1.11	1.10	1.10	1.07	1.07	1.09	1.09
Gd	4.17	4.22	4.55	4.69	4.62	4.38	4.39	4.65	4.95
Tb	0.69	0.69	0.70	0.71	0.70	0.68	0.67	0.70	0.71
Dy	3.87	3.92	3.89	4.11	3.94	3.98	3.86	3.97	4.02
Ho	0.83	0.84	0.84	0.89	0.86	0.83	0.80	0.83	0.85
Er	2.28	2.29	2.27	2.37	2.29	2.27	2.18	2.31	2.37
Tm	0.35	0.36	0.36	0.38	0.36	0.35	0.34	0.35	0.36
Yb	2.38	2.43	2.40	2.56	2.47	2.35	2.28	2.39	2.39
Lu	0.36	0.37	0.37	0.39	0.37	0.36	0.35	0.36	0.37
Hf	4.63	4.59	4.60	4.65	4.61	4.70	4.38	4.76	4.71

续表2

样品号	16T353	16T355	16T372	16T373	16T374	16T375	16T376	16T377	16T348
岩性	安山岩	英安岩							
SiO ₂	63.4	56.75	55.53	56.55	53.35	54.44	52.77	53.52	64.46
TiO ₂	0.70	0.98	0.85	0.84	0.83	0.84	0.85	0.83	0.68
Al ₂ O ₃	15.03	18.73	18.35	17.83	18.22	18.2	18.44	17.98	15.17
TFeO	3.75	4.00	6.76	5.52	5.48	6.26	7.00	5.46	3.44
TFe ₂ O ₃	4.17	4.45	7.50	6.13	6.08	6.95	7.77	6.06	3.82
MnO	0.11	0.16	0.18	0.07	0.14	0.12	0.16	0.12	0.1
MgO	1.03	0.63	3.84	1.86	1.91	2.33	4.01	2.76	0.91
CaO	4.54	9.76	2.74	4.49	5.43	5.58	3.78	6.21	4.04
Na ₂ O	4.09	3.96	4.8	4.84	6.69	5.1	4.79	3.65	4.06
K ₂ O	2.39	0.73	1.75	1.66	1.37	1.44	1.65	2.53	2.51
P ₂ O ₅	0.16	0.21	0.17	0.17	0.17	0.17	0.18	0.17	0.15
LOI	4.48	3.44	4.71	5.5	5.48	4.89	5.23	5.9	3.78
TOTAL	100.10	99.80	100.42	99.94	99.67	100.06	99.63	99.73	99.68
Li	72.10	10.80	79.10	62.70	61.50	109.00	77.40	76.20	67.50
Be	1.92	1.45	1.83	1.82	1.54	1.61	1.84	1.53	1.91
Sc	12.80	15.50	14.50	13.20	12.90	13.30	14.30	14.60	12.10
V	91.60	182.00	162.00	150.00	151.00	152.00	178.00	165.00	89.40
Cr	15.30	13.60	22.70	22.70	24.90	22.20	20.40	21.90	13.50
Co	9.94	8.11	21.40	15.50	18.00	18.70	22.20	19.80	9.06
Ni	6.14	9.41	9.23	9.49	10.30	10.40	9.73	11.00	5.57
Ga	16.90	16.10	20.20	17.90	18.10	18.60	20.20	19.00	16.90
Rb	60.80	18.60	58.10	54.30	40.10	41.80	53.00	67.90	61.70
Sr	180	359	491	329	461	312	464	341	193
Zr	237	153	183	181	179	183	191	185	262
Nb	9.83	8.89	8.96	9.2	8.89	8.99	9.37	9.17	9.94
Cs	3.8	1.87	3.8	6.02	2.76	7.06	3.31	8.36	3.76
Ba	585	279	536	417	414	484	406	611	668
Ta	0.77	0.67	0.66	0.67	0.64	0.74	0.69	0.66	0.75
Pb	26.20	8.86	38.30	7.59	3.45	6.98	8.98	18.10	31.60
Th	13.2	5.97	12.00	12.30	11.50	12.10	12.80	12.20	14.00
U	2.58	1.37	1.79	2.05	1.77	1.90	1.93	1.84	2.68
Y	24.80	23.80	23.80	24.40	21.80	24.50	26.10	24.10	25.10
Ti	4470	6369	5356	5261	5273	5269	5408	5373	4316
La	30.80	19.00	28.50	23.40	28.00	31.40	29.30	30.60	31.70
Ce	58.90	43.80	54.90	46.70	57.00	61.10	57.70	58.70	61.10
Pr	6.55	4.61	6.34	5.33	5.77	6.51	7.21	6.74	6.68
Nd	25.60	20.10	24.40	21.50	22.30	25.70	29.30	26.30	25.60
Sm	4.90	4.41	4.75	4.33	4.30	4.86	5.83	4.93	4.99
Eu	1.20	1.32	1.14	1.04	0.94	1.24	1.55	1.26	1.20
Gd	4.82	5.11	5.13	4.80	4.13	4.66	5.23	4.66	4.99
Tb	0.76	0.76	0.73	0.74	0.66	0.76	0.84	0.73	0.76
Dy	4.44	4.31	4.23	4.20	3.80	4.39	4.80	4.24	4.47
Ho	0.94	0.91	0.9	0.92	0.81	0.93	1	0.91	0.95
Er	2.62	2.46	2.49	2.56	2.24	2.50	2.68	2.46	2.65
Tm	0.41	0.39	0.39	0.41	0.35	0.39	0.42	0.39	0.41
Yb	2.7	2.68	2.67	2.78	2.42	2.62	2.79	2.69	2.79
Lu	0.41	0.42	0.42	0.43	0.37	0.4	0.42	0.4	0.43
Hf	6.31	4.35	5.08	5.09	5.08	5.18	5.28	5.13	6.53

续表2

样品号	16T349	16T350	16T351	16T352	18T303	18T304	18T305	18T306	18T307	18T308
岩性	英安岩									
SiO ₂	67.86	62.03	62.10	64.75	65.98	66.02	66.15	65.78	65.99	65.58
TiO ₂	0.65	0.72	0.71	0.73	0.54	0.53	0.54	0.52	0.53	0.52
Al ₂ O ₃	14.40	15.49	15.37	16.05	15.57	15.40	15.53	15.59	15.26	15.49
TFeO	2.82	3.61	3.81	3.61	3.93	3.80	3.83	3.75	3.82	3.90
TFe ₂ O ₃	3.13	4.01	4.23	4.01	4.36	4.22	4.26	4.17	4.25	4.33
MnO	0.08	0.12	0.12	0.08	0.06	0.07	0.07	0.07	0.07	0.07
MgO	0.52	1.29	1.11	0.95	1.93	1.91	1.90	1.84	1.87	1.92
CaO	2.99	4.17	4.40	2.47	3.19	3.45	3.34	3.16	3.49	3.65
Na ₂ O	4.91	4.73	4.42	6.40	3.47	3.36	3.47	3.18	3.24	3.13
K ₂ O	2.13	2.17	2.50	1.47	4.08	4.06	4.07	4.42	4.11	4.13
P ₂ O ₅	0.15	0.16	0.16	0.17	0.14	0.13	0.14	0.14	0.14	0.14
LOI	3.01	4.91	4.58	2.59	1.44	1.33	1.31	1.56	1.40	1.58
TOTAL	99.83	99.80	99.70	99.67	100.76	100.48	100.78	100.44	100.35	100.54
Li	50.90	60.80	67.70	49.50	13.05	12.90	15.02	15.48	12.92	16.64
Be	1.54	1.71	1.81	1.44	2.46	2.35	2.18	2.15	2.44	2.12
Sc	10.00	13.50	12.80	11.30	20.22	20.07	10.86	17.04	20.41	10.98
V	91.60	95.30	95.70	88.40	92.82	90.63	89.24	87.01	92.30	88.57
Cr	16.10	15.00	16.00	13.70	17.42	21.21	10.93	11.86	19.53	13.32
Co	4.63	8.58	9.62	10.60	17.90	16.40	15.40	13.70	16.40	13.90
Ni	5.67	5.61	5.96	7.87	7.03	11.91	5.92	7.01	6.97	5.76
Ga	13.20	16.40	16.80	14.10	14.98	14.69	17.73	18.20	14.88	18.58
Rb	39.70	47.40	59.30	36.20	101.04	100.61	145.07	156.26	100.90	154.13
Sr	186	160	180	182	336	315	303	290	317	302
Zr	206	259	261	278	243	255	234	211	247	236
Nb	9.32	10.30	10.20	10.50	20.20	19.80	12.90	12.80	20.10	12.80
Cs	2.70	3.09	4.06	2.62	2.14	2.07	2.13	1.52	2.04	1.97
Ba	576	464	639	290	778	692	687	792	701	754
Ta	0.75	0.84	0.83	0.81	1.28	1.25	1.21	1.20	1.31	1.23
Pb	12.00	14.50	27.60	12.10	10.73	10.59	10.35	11.06	10.75	9.88
Th	13.80	14.00	14.00	14.90	24.92	25.10	38.32	38.78	26.20	39.14
U	2.43	2.83	2.72	2.76	2.89	3.06	4.79	4.26	3.31	4.56
Y	23.40	26.60	27.10	25.20	29.19	28.02	25.24	24.77	28.68	25.62
Ti	4323	4660	4563	4626	3759	3627	3195	3156	3660	3240
La	29.40	34.00	34.20	25.60	55.86	56.51	48.94	51.12	57.84	53.03
Ce	58.30	62.00	63.90	50.00	104.92	104.58	90.48	93.82	107.08	98.53
Pr	6.51	6.81	7.04	5.65	11.47	11.49	10.14	10.39	11.65	10.96
Nd	25.10	26.10	26.90	22.10	38.75	38.95	34.25	35.01	39.56	37.27
Sm	4.85	4.93	5.17	4.57	6.65	6.59	5.92	6.08	6.71	6.40
Eu	0.97	1.18	1.27	0.99	0.91	0.84	1.21	1.37	0.86	1.31
Gd	4.64	4.81	4.80	4.64	5.58	5.58	5.59	5.74	5.63	5.95
Tb	0.73	0.80	0.79	0.75	0.57	0.56	0.81	0.79	0.56	0.83
Dy	4.18	4.66	4.73	4.38	4.47	4.28	4.48	4.48	4.40	4.66
Ho	0.88	0.98	0.99	0.92	0.70	0.66	1.00	0.98	0.67	1.03
Er	2.39	2.78	2.76	2.51	2.41	2.28	2.54	2.51	2.37	2.65
Tm	0.38	0.43	0.43	0.39	0.30	0.29	0.44	0.43	0.30	0.44
Yb	2.52	2.89	2.94	2.59	2.76	2.62	2.79	2.74	2.71	2.87
Lu	0.38	0.45	0.45	0.40	0.42	0.40	0.40	0.39	0.42	0.41
Hf	6.16	6.51	6.49	7.03	6.26	6.53	6.10	5.68	6.38	6.21

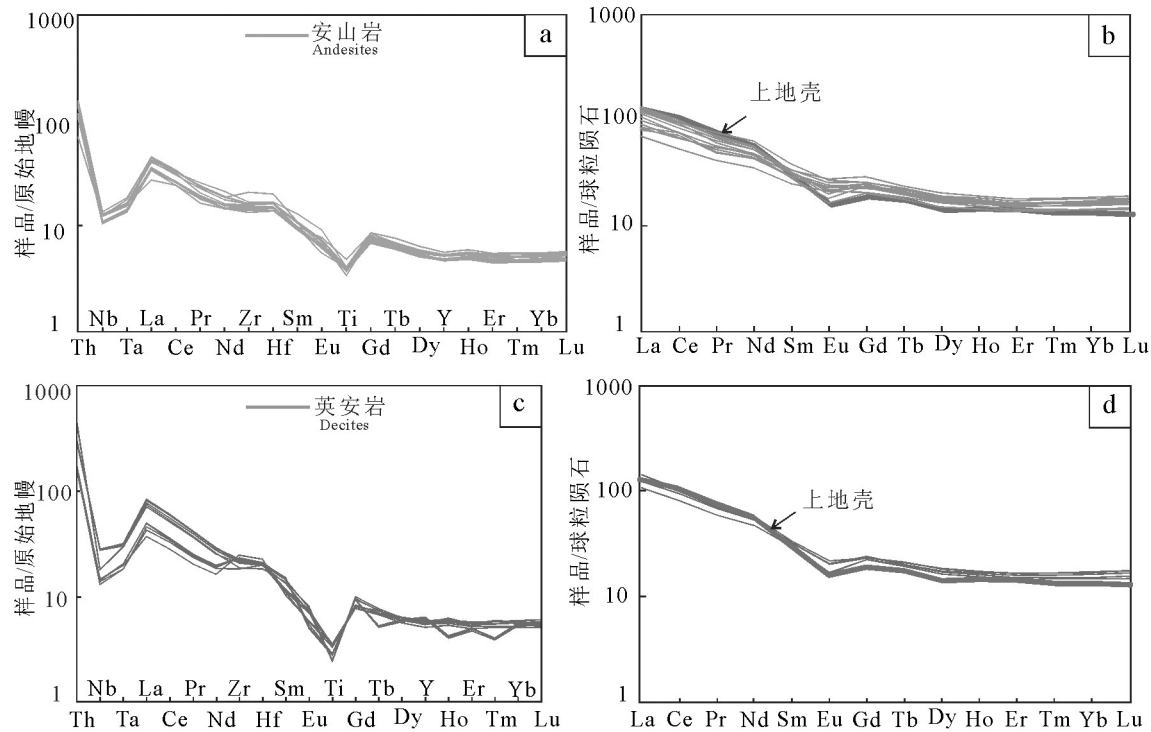


图5 西藏班戈县马前乡安山岩(a, b)和英安岩(c, d)的微量元素原始地幔标准化蛛网图和稀土元素球粒陨石标准化配分曲线
标准化数据和上地壳数据引自参考文献(据Sun and McDonough, 1989)

Fig.5 Primitive-mantle-normalized trace elements spidergrams and Chondrite-normalized rare-earth element patterns of the andesite (a, b) and dacites (c, d) in Maqian Town of Baingoin County, Tibet (Normalizing and upper crust data from reference, after Sun and McDonough, 1989)

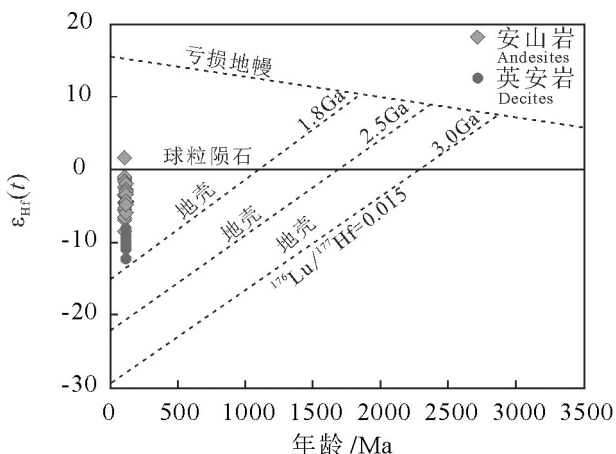


图6 西藏班戈县马前乡火山岩的 $\varepsilon_{\text{Hf}}(t)$ -U-Pb年龄图解
Fig.6 Plots of $\varepsilon_{\text{Hf}}(t)$ vs. U-Pb ages of the volcanic rocks in Maqian Town of Baingoin County, Tibet

动进行了较为详细的地球化学、年代学及同位素的研究,提出拉萨地块中北部地区在140~110 Ma可能一直处于与羌塘碰撞有关的同碰撞背景。

尽管前人已经获得了一些去申拉组火山岩的

年代学资料,但是主要集中于班公湖—怒江缝合带西段,中—东段的相关年代学资料仍然较少。本次研究样品采自班戈北部马前乡地区,位于班公湖—怒江缝合带中段。安山岩和英安岩样品中锆石具有明显的岩浆成因振荡环带,显示出明显岩浆锆石的特征。获得的锆石U-Pb年龄为105~114 Ma,代表了火山岩的岩浆结晶时代,即班戈北部马前乡地区去申拉组火山岩的形成时代为早白垩世,从而为去申拉组火山岩的准确时代提供了新的约束。

6.2 岩石成因与源区性质

对于长英质火山岩的成因,通常有2种解释:(1)起源于幔源基性岩浆经历广泛的结晶分异和同化混染作用(Bacon and Oruitt, 1988; Ingle et al., 2002);(2)来自幔源基性岩浆的热量促使地壳物质部分熔融的产物(Roberts and Clemens, 1993; Tepper et al., 1993)。第一种成因解释要求有大量的中—基性岩浆岩,这与研究区内并没有发现大规模同时代基性岩相悖。虽然本项研究发现了较多

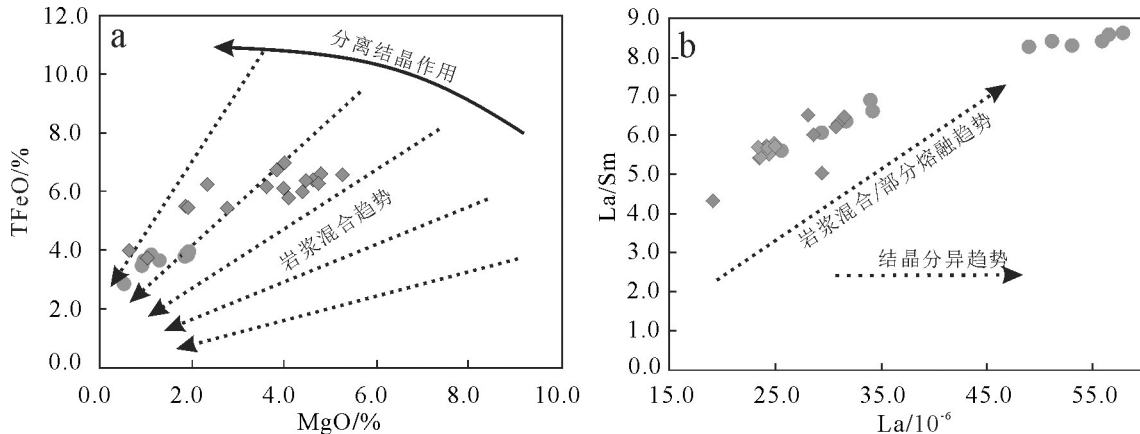


图7 西藏班戈县马前乡火山岩的MgO-TFeO图解(据Zorpi et al., 1989)(a)和La-La/Sm图解(据Schiano et al., 2010)(b)
Fig.7 MgO-TFeO (a) and La-La/Sm diagrams (b) (after Zorpi et al., 1989) and La-La/Sm diagrams (after Schiano et al., 2010) of the volcanic rocks in Maqian Town of Baingoin County, Tibet

的与英安岩($\varepsilon_{\text{Hf}}(t) = -12.3 \sim -8.1$)同时代的安山岩($\varepsilon_{\text{Hf}}(t) = -8.6 \sim +1.5$),但是它们具有明显不同的Hf同位素成分(图6),显示出其岩浆源区的差异。英安岩具有与上地壳类似的稀土和微量元素组成,由此推测它们应当是地壳物质部分熔融的产物。考虑到它们具有较古老的锆石二阶段Hf模式年龄($T_{\text{DM}^{\text{C}}} = 1748 \sim 1952 \text{ Ma}$),初步推测它们是古元古代地壳物质熔融的产物。

对于中性火山岩的成因,一般有以下几种解释:(1)幔源玄武质熔体的结晶分异作用(Sisson and Grove, 1993; Müntener et al., 2001);(2)被俯冲流体或熔体交代过的地幔楔橄榄岩的部分熔融(Tatsumi, 1982; McCarron and Smellie, 1998);(3)镁铁质中、下地壳岩石部分熔融(Smith and Leeman, 1987);(4)基性岩浆与酸性岩浆的岩浆混合(Heiken and Eichelberger, 1980)。本文倾向于最后一种解释,理由如下:首先,安山岩样品的锆石 $\varepsilon_{\text{Hf}}(t)$ 值($-8.6 \sim +1.5$)以负值为主,与幔源基性熔体结晶分异作用或者地幔楔橄榄岩部分熔融的产物,其成岩过程应当有地壳物质的参与;其次,安山岩样品具有变化范围较大的Mg[#]值(25~63),而中、下地壳岩石部分熔融形成的岩石通常只具有较低的(<40)的Mg[#]值(Smith and Leeman, 1987);再次,在TFeO-MgO和La-La/Sm图解(图7)上,安山岩显示出明显的岩浆混合趋势。本文报道的英安岩可能代表了岩浆混合中的酸性端元,而Zhu et al.

(2009)在拉萨地块北部报道的同时代幔源玄武安山岩则可能代表了基性端元,安山岩可能是这两类岩浆混合的产物。

6.3 构造意义

班公湖—怒江中特提斯洋的闭合时间一直缺乏准确的约束。部分学者把沿班公湖—怒江缝合带展布的早白垩世晚期(120~110 Ma)OIB型基性岩及其伴生的层状灰岩解释为洋岛岩石组合,进而由此推测此时班公湖—怒江缝合带仍未完全关闭(Zhu et al., 2006; Liu et al., 2014; Zhang et al., 2014; Fan et al., 2015)。然而,新近对班公湖—怒江缝合带上120~110 Ma基性岩进行的系统地球化学研究表明,这一期基性岩浆事件具有混合岩浆源区,分别为浅层的MORB型源区和深层的OIB型源区,与典型的洋岛环境具有一定差别(Zhu et al., 2015)。

通常认为,大洋板块俯冲环境下形成的岩浆岩主要为钙碱性系列岩石,而在随后的陆—陆碰撞阶段主要形成高钾钙碱性岩石(LeBas et al., 1986; Zhu et al., 2011; Hu et al., 2018, 2019)。已有研究资料表明,沿班公湖—怒江缝合带及其两侧出露大量113 Ma左右的岩浆岩(Zhu et al., 2011)。本次研究在马前乡地区识别出的早白垩世安山岩和英安岩的形成时代为107~114 Ma,与这些岩浆岩的时代基本一致。如前文所述,马前乡地区的早白垩世火山岩主要为高钾钙碱性系列岩石,它们与拉萨地块中北部的近同时代岩浆岩一致,其形成均与拉萨与南羌塘地块的陆—陆碰撞相关。因此,我们认为这些

表3 西藏班戈县马前火山岩的锆石Hf同位素分析结果

Table 3 Zircon Hf isotopic data of the volcanic rocks in the Maqianxiang area, Baingoin County, Tibet

样品号	年龄 t/Ma	$^{176}\text{Yb}/^{177}\text{Hf}$	$\pm 2\sigma$	$^{176}\text{Lu}/^{177}\text{Hf}$	$\pm 2\sigma$	$^{176}\text{Hf}/^{177}\text{Hf}$	$\pm 2\sigma$	$^{176}\text{Hf}/^{177}\text{Hf}_i$	$\varepsilon_{\text{Hf}}(0)$	$\varepsilon_{\text{Hf}}(t)$	$\pm 2\sigma$	T_{DM}/Ma	$T_{\text{DM}}^{\text{C}}/\text{Ma}$	$f_{\text{Lu/Hf}}$
安山岩														
16T337 03	107	0.047315	0.000548	0.001902	0.000016	0.282606	0.000043	0.282602	-5.9	-3.7	1.5	938	1399	-0.94
16T337 04	107	0.036741	0.000184	0.001492	0.000008	0.282670	0.000031	0.282667	-3.6	-1.4	1.1	836	1253	-0.96
16T337 05	107	0.020243	0.000116	0.000925	0.000005	0.282677	0.000031	0.282675	-3.4	-1.1	1.1	813	1235	-0.97
16T337 06	107	0.045701	0.000301	0.001831	0.000012	0.282605	0.000034	0.282602	-5.9	-3.7	1.2	937	1400	-0.94
16T337 07	107	0.062426	0.001318	0.002472	0.000050	0.282551	0.000034	0.282546	-7.8	-5.7	1.2	1033	1526	-0.93
16T337 08	107	0.033150	0.000164	0.001406	0.000008	0.282607	0.000029	0.282604	-5.8	-3.6	1.0	924	1395	-0.96
16T337 11	107	0.067902	0.000572	0.002735	0.000022	0.282663	0.000037	0.282657	-3.9	-1.7	1.3	876	1275	-0.92
16T337 12	107	0.039048	0.000752	0.001567	0.000023	0.282577	0.000039	0.282574	-6.9	-4.7	1.4	971	1463	-0.95
16T337 13	107	0.053782	0.000635	0.002086	0.000020	0.282512	0.000037	0.282508	-9.2	-7.0	1.3	1079	1612	-0.94
16T337 15	107	0.050608	0.000458	0.002016	0.000018	0.282610	0.000030	0.282606	-5.7	-3.5	1.0	936	1392	-0.94
16T337 16	107	0.035153	0.000298	0.001425	0.000010	0.282557	0.000032	0.282554	-7.6	-5.4	1.1	996	1507	-0.96
16T337 17	107	0.042507	0.000382	0.001735	0.000016	0.282466	0.000038	0.282463	-10.8	-8.6	1.3	1134	1712	-0.95
16T337 19	107	0.026859	0.000118	0.001247	0.000006	0.282752	0.000029	0.282749	-0.7	1.5	1.0	714	1069	-0.96
16T337 21	107	0.044693	0.000667	0.001768	0.000018	0.282520	0.000047	0.282517	-8.9	-6.7	1.7	1057	1591	-0.95
16T337 23	107	0.020197	0.000497	0.000936	0.000024	0.282638	0.000045	0.282636	-4.7	-2.5	1.6	869	1323	-0.97
英安岩														
18T303-1	113	0.027198	0.000346	0.000933	0.000011	0.282425	0.000019	0.282424	-12.3	-9.8	0.7	1167	1796	-0.97
18T303-2	113	0.033509	0.000455	0.001182	0.000015	0.282474	0.000019	0.282472	-10.5	-8.1	0.7	1106	1688	-0.96
18T303-3	113	0.035136	0.000616	0.001213	0.000022	0.282418	0.000020	0.282416	-12.5	-10.1	0.7	1186	1814	-0.96
18T303-4	113	0.042879	0.000637	0.001454	0.000022	0.282423	0.000019	0.282420	-12.4	-10.0	0.7	1187	1805	-0.96
18T303-5	113	0.023231	0.000478	0.000812	0.000016	0.282428	0.000021	0.282426	-12.2	-9.8	0.8	1160	1790	-0.98
18T303-6	113	0.026664	0.000123	0.000938	0.000006	0.282409	0.000020	0.282407	-12.9	-10.4	0.7	1191	1834	-0.97
18T303-7	113	0.069180	0.001157	0.002280	0.000050	0.282426	0.000026	0.282421	-12.2	-9.9	0.9	1209	1800	-0.93
18T303-8	113	0.029024	0.000335	0.001006	0.000018	0.282430	0.000020	0.282428	-12.1	-9.7	0.7	1163	1786	-0.97
18T303-9	113	0.027699	0.000973	0.000942	0.000030	0.282431	0.000020	0.282429	-12.1	-9.7	0.7	1160	1784	-0.97
18T303-10	113	0.024061	0.000229	0.000835	0.000006	0.282447	0.000020	0.282445	-11.5	-9.1	0.7	1134	1748	-0.97
18T303-11	113	0.026720	0.000254	0.000937	0.000005	0.282410	0.000021	0.282408	-12.8	-10.4	0.7	1189	1831	-0.97
18T303-12	113	0.034427	0.000418	0.001170	0.000018	0.282424	0.000020	0.282422	-12.3	-9.9	0.7	1176	1800	-0.96
18T303-13	113	0.045284	0.000278	0.001519	0.000005	0.282407	0.000021	0.282404	-12.9	-10.5	0.7	1212	1840	-0.95
18T303-14	113	0.030543	0.000772	0.001023	0.000020	0.282395	0.000021	0.282393	-13.3	-10.9	0.7	1212	1864	-0.97
18T303-15	113	0.037882	0.000544	0.001255	0.000015	0.282356	0.000019	0.282354	-14.7	-12.3	0.7	1275	1952	-0.96
安山岩														
18T097-1	113	0.046978	0.000853	0.001920	0.000031	0.282629	0.000019	0.282625	-5.0	-2.7	0.7	904	1343	-0.94
18T097-2	113	0.031650	0.000275	0.001169	0.000014	0.282658	0.000018	0.282655	-4.0	-1.7	0.6	846	1277	-0.96
18T097-3	113	0.032283	0.000587	0.001183	0.000015	0.282599	0.000024	0.282597	-6.1	-3.7	0.8	929	1408	-0.96
18T097-4	113	0.037659	0.000691	0.001348	0.000019	0.282635	0.000019	0.282632	-4.9	-2.5	0.7	883	1329	-0.96
18T097-5	113	0.027013	0.000641	0.000999	0.000019	0.282620	0.000024	0.282618	-5.4	-3	0.8	896	1361	-0.97
18T097-6	113	0.032371	0.000265	0.001178	0.000011	0.282585	0.000017	0.282583	-6.6	-4.2	0.6	949	1439	-0.96
18T097-7	113	0.059502	0.000719	0.002431	0.000017	0.282578	0.000026	0.282573	-6.9	-4.6	0.9	993	1461	-0.93
18T097-8	113	0.057588	0.000784	0.002270	0.000024	0.282628	0.000020	0.282623	-5.1	-2.8	0.7	915	1348	-0.93
18T097-9	113	0.027968	0.000242	0.001012	0.000004	0.282583	0.000023	0.282581	-6.7	-4.3	0.8	947	1443	-0.97
18T097-10	113	0.034431	0.000628	0.001219	0.000018	0.282545	0.000020	0.282542	-8.0	-5.7	0.7	1008	1530	-0.96
18T097-11	113	0.036596	0.000235	0.001338	0.000010	0.282613	0.000020	0.282611	-5.6	-3.2	0.7	913	1377	-0.96
18T097-12	113	0.038589	0.000183	0.001420	0.000010	0.282588	0.000022	0.282585	-6.5	-4.1	0.8	951	1434	-0.96
18T097-13	113	0.047550	0.000401	0.001706	0.000010	0.282574	0.000022	0.282571	-7.0	-4.6	0.8	978	1466	-0.95

岩浆岩的大规模产出可以推测班公湖—怒江缝合带在早白垩世就已经闭合。这一推断也得到了古地测资料的支持。在110~50 Ma之间,拉萨地块南缘的古纬度为 $\sim 20 \pm 4^\circ\text{N}$ (Lippert et al., 2014)。考虑到此时拉萨地块应当具有600 km左右的宽度,拉萨地块北缘的古纬度可能为 $\sim 26 \pm 4^\circ\text{N}$,与此时南羌塘地块南缘的古纬度($29.3 \pm 5.7^\circ\text{N}$)误差范围内部分重合(Chen et al., 2014),从而指示此时陆—陆碰撞可能已经发生。班公湖—怒江缝合带内120~108 Ma玄武岩的地球化学数据指向混合地幔源区,并且这些玄武岩可能来源于拉萨—羌塘碰撞后软流圈物质的减压熔融(Zhu et al., 2016)。构造填图和碎屑锆石研究也表明,南羌塘地块在晚侏罗世—早白垩世发生了非常明显的地壳缩短,其缩短程度甚至可以与新生代的印度—欧亚大陆碰撞相对比(Raterman et al., 2014)。班公湖—怒江缝合带中段尼玛县的沉积学研究表明:在125~118 Ma该地区沉积环境就已由海相转化为陆相,这与拉萨与南羌塘地块陆—陆碰撞事件相关(Kapp et al., 2007)。

7 结 论

(1)班公湖—怒江缝合带中段马前乡地区的安山岩和英安岩的形成时代为105~114 Ma,揭示了去申拉组火山岩的形成时代为早白垩世。

(2)安山岩富集Th和U,亏损Nb、Ta和Ti,具有变化范围较大的Mg[#]值(25~63),锆石 $\varepsilon_{\text{Hf}}(t)$ 值(-8.6~+1.5)也以负值为主,应当为幔源镁铁质熔体与壳源熔体的混合产物。英安岩具有与安山岩类似的微量元素成分特征,以及负的锆石 $\varepsilon_{\text{Hf}}(t)$ 值(-12.3~-8.1),应当是地壳部分熔融的产物。

(3)马前乡地区早白垩世火山岩支持班公湖—怒江中特提斯洋的闭合时间为早白垩世,此时拉萨与南羌塘地块已经发生了陆—陆碰撞。

致谢:锆石LA-ICP-MS U-Pb定年和Hf同位素分析得到了中国地质科学院矿产资源研究所侯可军副研究员的帮助,在此致以衷心的感谢。

References

- Bacon C R, Oruitt T H. 1988. Compositional evolution of the zoned cal-calkaline magma chamber of mount Mazama, Crater Lake, Oregon[J]. Contribution to Mineralogy and Petrology, 98: 224–256.
- Chen Weiwei, Zhang Shihong, Ding Jikai, Zhang Junhong, Zhao Xixi, Zhu Lidong, Yang Wenguang, Yang Tiansui, Li Haiyan, Wu Huachun. 2017. Combined paleomagnetic and geochronological study on Cretaceous 1 strata of the Qiangtang terrane, central Tibet[J]. Gondwana Reserach, 241: 373–389.
- Chen Yulu, Jiang Yuansheng. 2002. Age and significance of volcanic rock of Early Cretaceous in the Ban Ge—Qielicuo areaa in Tibet [J]. Journal of Geomechanics, 8(1): 43–49.
- Fan Jianjun, Li Cai, Xie Chaoming, Wang Ming, Chen Jingwen. 2015. Petrology and U-Pb zircon geochronology of bimodal volcanic rocks fromthe Maierze Group, northern Tibet: Constraints on the timing of closure of the Banggong—Nujiang Ocean[J]. Lithos, 227: 148–160.
- Fan Jianjun, Li Cai, Xie Chaoming, Wang Ming. 2014. Petrology, geochemistry, and geochronology of the Zhonggang ocean island, northern Tibet: Implications for the evolution of the Bang gong co-Nujiang oceanic arm of Neo-Tethys[J]. International Geology Review, 56: 1504–1520.
- Girardeau J, Marcoux J, Allegre C J, Bassoulet J P, Tang Youking, Xiao Xuchang, Zao Yougong, Wang Xibin. 1984. Tectonic environment and geodynamic significance of the Neo-Cimmerian Donqiao ophiolite, Bangong— Nujiang suture zone, Tibet[J]. Nature, 307: 27–31.
- Guynn J H, Kapp P, Pullen A, Heizler M, Gehrels G, Lin D. 2006. Tibetan basement rocks near Amdo reveal “missing” Mesozoic tectonism along the Bangong suture, central Tibet [J]. Geology, 34: 505–508.
- Hastie A R, Kerr A C, Pearce J A, Mitchell S F. 2007. Classification of altered volcanic island arc rocks using immobile trace elements: development of the Th-Co discrimination diagram[J]. Journal of Petrology, 48: 2341–2357.
- Heiken G, Eichelberger J C. 1980. Eruptions at Chaos Crags, Lassen Volcanic National Park, California[J]. Volcanology and Geothermal Research, 7: 443–481.
- Hou Kejun, Li Yanhe, Tian Youyong. 2009. In situ U-Pb zircon dating using laser ablation– multi ion counting– ICP– MS[J]. Mineral Deposits, 28(4): 481–492(in Chinese with English abstract).
- Hou Zengqian, Mo Xuanxue, Yang Zhiming, Wang Anjian, Pan Guitang, Qu Xiaoming, Nie Fengjun. 2006. Metallogenesis in the collisional orogen of the Qinghai–Tibet Plateau: Tectonic setting, tempo– spatial distribution and ore deposit types[J]. Geology in China, 33(2): 341–351(in Chinese with English abstract).
- Hou Zengqian, Zhong Dalai, Deng Wanming. 2004. A tectonic model for porphyry copper–molybdenum–gold metallogenic belts on the eastern margin of the Qinghai–Tibet Plateau[J]. Geology in China, 31(1): 1–14.
- Hu Peiyuan, Zhai Qingguo, Jahn Bor-ming, Wang Jun, Li Cai, Chung Sunli, Lee Haoyang, Tang Suohan. 2017. Late early cretaceous magmatic rocks (118– 113 Ma) in the middle segment of the Banggong— Nujiang suture zone, Tibetan plateau: Evidence of

- lithospheric delamination[J]. *Gondwana Research*, 44: 116–138.
- Hu Peiyuan, Zhai Qingguo, Wang Jun, Tang Yue, Wang Haitao, Hou Kejun. 2018. Ediacaran magmatism in the North Lhasa terrane, Tibet and its tectonic implications[J]. *Precambrian Research*, 307: 137–154.
- Ingle S, Weis D, Frey F A. 2002. Indian continental Crust recovered from Elan Bank, Kerguelen Plateau(ODP Leg 183, Site 1137) [J]. *Journal of Petrology*, 43(7): 1241–1257.
- Jackson S E, Pearson N J, Griffin W L, Belousova E A. 2004. The application of laser ablation– inductively coupled plasma– mass spectrometry to in situ U– Pb zircon geochronology[J]. *Chemical Geology*, 211: 47–69.
- Kapp P, DeCelles P G, Gehrels G E, Ding L. 2007. Geological records of the Lhasa– Qiangtang and Indo– Asian collisions in the Nima area of central Tibet[J]. *Geological Society of America Bulletin*, 119: 917–932.
- LeBas M J L, Streckeisen A L. 1991. The IUGS systematics of igneous rocks[J]. *Journal of the Geological Society*, 148(5): 825–833.
- Leier A L, Decelles P G, Kapp P, Gehrels G E. 2007. Lower Cretaceous strata in the Lhasa Terrane, Tibet, with implications for understanding the early tectonic history of the Tibetan Plateau[J]. *Sedimentary Research*, 77: 809–825.
- Li Haibing, Vauj F, Xu Zhiqin, Yang Jingsui, Tapponnier P, Lacassin R, Chen Songyong, Qi Xuexiang, Chevalier M L. 2006. Deformation and tectonic evolution of the Karakorum falut, western Tibet[J]. *Geology in China*, 33(2): 239– 255(in Chinese with English abstract).
- Lippert P C, van Hinsbergen D J J, Dupont– Nivet G. 2014. Early Cretaceous to present latitude of the central proto– Tibetan Plateau: A paleomagnetic synthesis with implications for Cenozoic tectonics, paleogeography, and climate of Asia[J]. *Geology Society of America Special Paper*, 507: 1–21.
- Liu Min, Zhu Dicheng, Zhao Zhdan, Mo Xuanxue, Guan Qi, Zhang Liangliang, Yu Feng, Liu Meihua. 2010. Magma mixing of Late Early Jurassic age from Nyainrong, northern Tibet and its tectonic significance[J]. *Acta Petrologica Sinica*, 26: 3117–3130(in Chinese with English abstract).
- Liu Weiliang, Huang Qiangtai, Gu Man, Zhong Yun, Zhou Renjie, Gu Xiaodong, Zheng Hao, Liu Jingnan, Lu Xingxin, Xia Bin. 2018. Origin and tectonic implications of the Shiquanhe high– Mg andesite, western Bangong suture, Tibet[J]. *Gondwana Research*, 60: 1–14.
- Liu Weiliang, Xia Bin, Zhong Yun, Cai Jiaxin, Li Jianfeng, Liu Fenghong, Cai Zhourong, Sun Zhilei. 2014. Age and composition of the Rebang Co and Julu ophiolites, central Tibet: implications for the evolution of the Bangong Meso– Tethys[J]. *International Geology Review*, 56: 430–447.
- Ludwig K R. 2003. ISOPLOT 3: ageochronological toolkit for Microsoft excel[J]. Berkeley Geochronology Centre Special Publication, 4: 74.
- Matte P, Tapponnier P, Arnaud N, Bourjot L, Avouac J P, Vidal P, Liu Q, Pan Y S, Wang Y. 1996. Tectonics of Western Tibet, between the Tarim and the Indus[J]. *Earth and Planetary Science Letters*, 142: 311–330.
- McCarron J J, Smellie J L. 1998. Tectonic implications of fore– arc magmatism and generation of high– magnesian andesites: Alexander Island, Antarctica[J]. *Journal of the Geological Society, London*, 155: 269–280.
- Muntener O, Kelemen P B, Grove T L. 2001. The role of H₂O during crystallisation of primitive arc magmas under uppermost mantle conditions and genesis of igneous pyroxenites: An experimental study[J]. *Contributions to Mineralogy and Petrology*, 141: 643–658.
- Raterman N S, Robinson A C, Cowgill E S. 2014. Structure and detrital zircon geochronology of the Domar fold– thrust belt: Evidence of pre– Cenozoic crustal thickening of the western Tibetan Plateau[J]. *Geology Society of America Special Paper*, 507: 89–114.
- Roberts M P, Clemens J D. 1993. Origin of high– potassium calc– alkaline I–type granitoids[J]. *Geology*, 21(9): 825–828.
- Schiano P, Monziger M, Eissen J P, Martin H, Koga K T. 2010. Simple mixing as the major control of the evolution of volcanic suites in the Ecuadorian Andes[J]. *Contributions to Mineralogy and Petrology*, 160: 297–312.
- Sisson T W, Grove T L. 1993. Experimental investigations of the role of H₂O in calc– alkaline differentiation and subduction zone magmatism[J]. *Contributions to Mineralogy and Petrology*, 113: 143–166.
- Smith D R, Leeman W P. 1987. Petrogenesis of Mount St. Helens dacitic magmas[J]. *Geophysical Research*, 92: 10313–10334.
- Sun S S, McDonough W F. 1989. Chemical and isotopic systematics of oceanic basalts: Implications for mantle composition and processes[J]. *Geological Society Special Publication*, 42: 313–345.
- Tatsumi Y. 1982. Origin of high– magnesian andesites in the Setouchi volcanic belt, southwest Japan, II. Melting phase relations at high pressures[J]. *Earth and Planetary Science Letters*, 60: 305–317.
- Tepper J H, Nelson B K, Bergantz G W, Irving A J. 1993. Petrology of the Chilliwack batholith, North Cascades, Washington: Generation of calc– alkaline graptolites by melting of mafic lower crust with variable water fugacity[J]. *Contribution to Mineralogy and Petrology*, 113: 333–351.
- Winchester J A, Floyd P A. 1977. Geochemical discrimination of different magma series and their differentiation products using immobile elements[J]. *Chemical Geology*, 20: 325–343.
- Wu Fuyuan, Yang Yueheng, Xie Liewen, Yang Jinhu, Xu Ping. 2006. Hf isotopic compositions of the standard zircons and baddeleyites used in U– Pb geochronology[J]. *Chemical Geology*, 234: 105–126.
- Wu Hao, Li Cai, Hu Peiyuan, Fan Jianjun, Zhang Hongyu, Li Jiao.

2013. The discovery of Qushenla volcanic rocks in Tasepule area of Nyima Country, Tibet, and its geological significance[J]. Geological Bulletin of China, 32(7): 1014–1026(in Chinese with English abstract).
- Wu Hao, Li Cai, Xu Mengjing, Li Xingkai. 2015. Early Cretaceous adakitic magmatism in the Dachagou area, northern Lhasa terrane, Tibet: Implications for slab roll-back and subsequent slab break-off of the lithosphere of the Bangong–Nujiang Ocean[J]. Journal of Asian Earth Sciences, 97: 51–66.
- Xu Ronghua, Schärer U, Allègre C J. 1985. Magmatism and metamorphism in the Lhasa block (Tibet): A Geochronological study[J]. The Journal of Geology, 93: 41–57.
- Xu Zhiqin, Yang Jingsui, Hou Zengqian, Zeng Lingsen, Li Haibing, Zhang Jianxin, Li Zhonghai, Ma Xuxuan. 2016. The progress in the study of continental dynamics of the Tibetan Plateau[J]. Geology in China, 43(1): 1–42(in Chinese with English abstract).
- Xu Zhiqin, Yang Jingsui, Li Haibing, Zhang Jianxin, Zeng Lingsen, Jiang Mei. 2006. The Qinghai–Tibet plateau and continental dynamics: A review on terrain tectonics, collisional orogenesis, and processes and mechanisms for the rise of the plateau[J]. Geology in China, 33(2): 222–238(in Chinese with English abstract).
- Yang Jingsui, Wang Xibin, Shi Rendeng, Xu Zhiqin, Wu Cailai. 2004. The Durngoi ophiolite in East Kunlun, northern Qinghai–Tibet Plateau: a fragment of paleo–Tethyan oceanic crust[J]. Geology in China, 31(3): 226–229(in Chinese with English abstract).
- Zhang Kaijun, Xia Bin, Zhang Yuxiu, Liu Weiliang, Zeng Lu, Li Jianfeng, Xu Lifeng. 2014. Central Tibetan Meso–Tethyan oceanic plateau[J]. Lithos, 210–211: 278–288.
- Zhang Kaijun, Xia Bangdong, Wang Guanmin, Li Yongtie. 2004. Early Cretaceous stratigraphy, depositional environments, sandstone provenance, and tectonic setting of central Tibet, western China[J]. Geological Society of America Bulletin, 116: 1202–1222.
- Zhao Hui, Yang Jingsui, Liu Fei, Xiong Fahui, Zhang Lan, Lian Dongyang. 2015. Geochemical and chronological studies of the alkaline basalt in Saga along the Yarlung Zangbo suture zone, Tibet[J]. Geology in China, 42(5): 1242–1256(in Chinese with English abstract).
- Zhu Dichen, Li Shimin, Cawood Peter A, Wang Qing, Zhao Zhidan, Liu Shengao, Wang Liquan. 2016. Assembly of the Lhasa and Qiangtang terranes in central Tibet by divergent double subduction[J]. Lithos, 245: 7–17.
- Zhu Dichen, Mo Xuanxue, Niu Yaoling, Zhao Zhidan, Wang Liquan, Liu Yongsheng, Wu Fuyuan. 2009. Geochemical investigation of Early Cretaceous igneous rocks along an east–west traverse throughout the central Lhasa Terrane, Tibet[J]. Chemical Geology, 268: 298–312.
- Zhu Dichen, Pan Guitang, Mo Xuanxue, Wang Liquan, Liao Zhongli, Dong Guochen, Zhou Changyong. 2006. Late Jurassic–Early Cretaceous geodynamic setting in middle–northern Gangdese: New insights from volcanic rocks[J]. Acta Petrologica Sinica, 22(3): 534–546(in Chinese with English abstract).
- Zhu Dichen, Wang Qing, Zhao Zhidan, Chung Sunli, Cawood Peter A, Liu Shengao, Wu Fuyuan, Mo Xuanxue. 2015. Magmatic record of India–Asia collision[J]. Scientific Reports, 5: 14289.
- Zhu Dichen, Zhao Zhidan, Niu Yaoling, Mo Xuanxue, Chung Sunlin, Hou Zengqian, Wang Liquan, Wu Fuyuan. 2011. The Lhasa Terrane: Record of a microcontinent and its histories of drift and growth[J]. Earth and Planetary Science Letters, 301: 241–255.
- Zorpi M J, Coulon C, Orsini J B, Cocirat C. 1989. Magmamingling, zoning and emplacement in calc–alkaline granitoid plutons[J]. Tectonophysics, 157: 315–329.
- ### 附中文参考文献
- 陈玉禄, 江元生. 2002. 西藏班戈一切里错地区早白垩世火山岩的时代确定及意义[J]. 地质力学学报, 8(1): 43–49.
- 侯可军, 李延河, 田有荣. 2009. LA–MC–ICP–MS 锆石微区原位U–Pb定年技术[J]. 矿床地质, 28(4): 481–492.
- 侯增谦, 莫宣学, 杨志明, 王安建, 潘桂棠, 曲晓明, 聂凤军. 2006. 青藏高原碰撞造山带成矿作用: 构造背景、时空分布和主要类型[J]. 中国地质, 33(2): 341–351.
- 侯增谦, 钟大赉, 邓万明. 2004. 青藏高原东缘斑岩铜钼金成矿带的构造模式[J]. 中国地质, 31(1): 1–14.
- 李海兵, Franck Vauj, 许志琴, 杨经绥, Paul Tapponnier, Robin Lacassin, 陈松永, 戚学祥, Marie—Luce Chevalier. 2006. 喀喇昆仑断裂的变形特征及构造演化[J]. 中国地质, 33(2): 239–255.
- 吴浩, 李才, 胡培远, 范建军, 张红雨, 李娇. 2013. 西藏尼玛县塔色普勒地区去申拉组火山岩的发现及其地质意义[J]. 地质通报, 32(7): 1014–1026.
- 许志琴, 杨经绥, 侯增谦, 张泽明, 曾令森, 李海兵, 张建新, 李忠海, 马绪宣. 2016. 青藏高原大陆动力学研究若干进展[J]. 中国地质, 43(1): 1–42.
- 许志琴, 杨经绥, 李海兵, 张建新, 曾令森, 姜枚. 2006. 青藏高原与大陆动力学–地体拼合、碰撞造山及高原隆升的深部驱动力[J]. 中国地质, 33(2): 222–238.
- 杨经绥, 王希斌, 史仁灯, 徐志琴, 吴才来. 2004. 青藏高原北部东昆仑南缘德尔尼蛇绿岩: 一个被支解了的古特提斯洋壳[J]. 中国地质, 31(3): 226–229.
- 赵慧, 杨经绥, 刘飞, 熊发挥, 张岚, 连东洋. 2015. 西藏雅鲁藏布江缝合带萨嘎碱性玄武岩地球化学和年代学研究[J]. 中国地质, 42(5): 1243–1256.
- 朱弟成, 潘桂棠, 莫宣学, 王立全, 廖忠礼, 赵志丹, 董国臣, 周长勇. 2006. 冈底斯中北部晚侏罗世—早白垩世地球动力学环境: 火山岩约束[J]. 岩石学报, 22(3): 534–546.